The Journal of Immunology

RESEARCH ARTICLE | APRIL 01 2022

Combinatorial Expression of NK Cell Receptors Governs Cell Subset Reactivity and Effector Functions but Not Tumor Specificity FREE

Yamila Rocca; ... et. al

J Immunol (2022) 208 (7): 1802–1812.
https://doi.org/10.4049/jimmunol.2100874

Combinatorial Expression of NK Cell Receptors Governs Cell Subset Reactivity and Effector Functions but Not Tumor Specificity

Yamila Rocca,*,† Kevin Pouxvielh,* Marie Marotel,* Sarah Benezech,* Baptiste Jaeger,‡,§,1 Omran Allatif,* Nathalie Bendriss-Vermare,† Antoine Marçais,* and Thierry Walzer*

NK cell receptors allow NK cells to recognize targets such as tumor cells. Many of them are expressed on a subset of NK cells, independently of each other, which creates a vast diversity of receptor combinations. Whether these combinations influence NK cell antitumor responses is not well understood. We addressed this question in the C57BL/6 mouse model and analyzed the individual effector response of 444 mouse NK cell subsets, defined by combinations of 12 receptors, against tumor cell lines originating from different tissues and mouse strains. We found a wide range of reactivity among NK subsets, but the same hierarchy of responses was observed for the different tumor types, showing that the repertoire of NK cell receptors does not encode for different tumor specificities but for different intrinsic reactivities. The coexpression of CD27, NKG2A, and DNAM-1 identified subsets with relative cytotoxic specialization, whereas reciprocally, CD11b and KLRG1 defined the best IFN-γ producers. The expression of educating receptors Ly49C, Ly49I, and NKG2A was also strongly correlated with IFN-γ production, but this effect was suppressed by unengaged receptors Ly49A, Ly49F, and Ly49G2. Finally, IL-15 coordinated NK cell effector functions, but education and unbound inhibitory receptors retained some influence on their response. Collectively, these data refine our understanding of the mechanisms governing NK cell reactivity, which could help design new NK cell therapy protocols. ***The Journal of Immunology*****, 2022, 208: 1802–1812.**

Natural killer cells are innate lymphocytes that contribute to cancer immunosurveillance through target cell killing and cytokine secretion (1). The triggering of NK cell effector functions is controlled by inhibitory and activating NK cell receptors expressed at the cell surface. These receptors are evolutionarily very diverse. Activating NK cell receptors notably include NKG2D, DNAM-1, NKp30, NKp46, and CD16, whereas inhibitory NK cell receptors include many human killer cell Ig-like receptors and a large subset of Ly49s (mouse), NKG2A, KLRG1, and others. Upon interaction with other cells, the balance between activating and inhibitory signals governs the NK cell response (i.e., ignorance or activation and killing) (2). Many inhibitory NK cell receptors bind to MHC class I (MHC-I) molecules, and MHC-I–deficient cells are therefore recognized and killed by NK cells. Tumor recognition also involves activating ligands for which expression is induced upon oncogenic stress, such as NKG2D ligands, NKp30 ligands, or DNAM-1 ligands (3).

NK cell responsiveness against tumors is developmentally regulated; $CD11b^+$ mature NK cells are more cytotoxic than their immature $CD11b^-$ counterpart (4, 5), which is associated with transcriptional changes in the expression of multiple genes involved in NK cell cytotoxicity (6). NK cell reactivity is also regulated through a process independent of maturation and transcription (7) called NK cell education, during which chronic engagement of inhibitory NK cell receptors by self-MHC molecules maintains NK cell reactivity downstream, activating NK cell receptors (8). NK cell education requires inhibitory NK cell receptor signaling through ITIMs (9) and phosphatases, such as Src homology region 2 domain-containing phosphatase 1 (SHP-1) (10), and is associated with a higher basal activity of the mammalian target of rapamycin (mTOR)/Akt pathway, commensurate to the number of educating receptors expressed (11) and remodeling of secretory lysosomes (12). Lastly, NK cell reactivity is tuned by cytokines that either increase it (e.g., IL-2, IL-15, IL-12/IL-18, or IL-21) (13) or decrease it (e.g., TGF-β) (14, 15), which mechanistically involves JAK/STAT pathways (13) but also the regulation of mTOR activity (14, 16). In particular, IL-15 enhances NK cell killing activity (13) by upregulating the cytotoxic machinery (17) and by preactivating the LFA1 integrin (18) in an

*Centre International de Recherche en Infectiologie, INSERM U1111, Ecole Normale Supérieure de Lyon, Université Lyon 1, CNRS, UMR 5308, Lyon, France; †Centre de Recherche en Cancérologie de Lyon, INSERM U1052, CNRS UMR 5286, Centre Léon Bérard, Université Claude Bernard Lyon 1, Lyon, France; ‡Faculty of Medicine, Brain Research Institute, University of Zurich, Zurich, Switzerland; and §Faculty of Science, Brain Research Institute, University of Zurich, Zurich, Switzerland

[1]Current address: Genentech Research and Early Development, San Francisco, CA.

ORCIDs: 0000-0002-9587-3896 (S.B.); 0000-0001-8728-797X (B.J.); 0000-0002-8771-3585 (N.B.-V.); 0000-0002-3591-6268 (A.M.); 0000-0002-0857-8179 (T.W.).

Received for publication September 10, 2021. Accepted for publication January 28, 2022.

The laboratory of T.W. is supported by the Agence Nationale de la Recherche (ANR GAMBLER to T.W. and ANR JC BaNK to A.M.), the Association pour la Recherche sur le Cancer Foundation (Équipe Labellisée until 2018), the Ligue Nationale contre le Cancer (Équipe Labellisée since 2019), and the Institut National du Cancer (PLBio 2016-160 to A.M. and PLBio Reclaim to T.W.) and receives institutional grants from INSERM, CNRS, Université Claude Bernard Lyon 1, and École Normale Supérieure de Lyon.

Y.R.: conceptualization, formal analysis, investigation, methodology, writing (original draft), and writing (review and editing); K.P.: formal analysis and investigation; B.J.: formal analysis; O.A.: formal analysis; M.M.: formal analysis, investigation, and writing (review and editing); S.B.: formal analysis and investigation; N.B.-V.: resources and writing (review and editing); A.M.: conceptualization, supervision, funding acquisition, project administration, and writing (review and editing); T.W.: conceptualization, supervision, funding acquisition, writing (original draft), project administration, and writing (review and editing).

Address correspondence and reprint requests to Dr. Thierry Walzer and Dr. Antoine Marçais, Centre International de Recherche en Infectiologie, INSERM U1111–CNRS UMR5308, Université Lyon 1, ENS de Lyon, 21 Avenue Tony Garnier, 69365 Lyon Cedex 07, France. E-mail addresses: thierry.walzer@inserm.fr (T.W.) and antoine.marcais@inserm.fr (A.M.)

The online version of this article contains supplemental material.

Abbreviations used in this article: GzmB, granzyme B; MHC-I, MHC class I; mTOR, mammalian target of rapamycin; SHP-1, Src homology region 2 domain-containing phosphatase 1; tSNE, *t*-distributed stochastic neighbor embedding.

mTOR-dependent way (11). Thus, NK cell reactivity is regulated through multiple processes not necessarily coordinated, and our understanding of it is only partial (19, 20).

Many NK cell receptors are expressed in a variegated manner, which creates a large diversity in the NK cell population, with an estimated number of 6,000 to 30,000 subsets within a given individual (21), whereas the TCR repertoire was estimated in an order of magnitude of 10^6 (22). This diversity is shaped by differentiation, by self-MHC molecules, and by viral infections (19, 23, 24). In particular, CMV infection leads to the specific expansion of NK cell subsets expressing the activating receptors NKG2C in humans (25, 26) and Ly49H in mice (27, 28), and inhibitory NK cell receptors interactions with self-MHC molecules positively influence these expansions (29). These observations suggest that NK cell diversity could be important to allow an adaptive-like control of different viral infections, as recently reviewed (26). Whether NK cell diversity may also be relevant for the control of different tumor types remains an open question. In fact, there are a great variety of tumor types, with different patterns of ligands for NK cell receptors (3, 30–32), which could trigger specific NK cell subsets. This point has not been addressed using high-resolution techniques. To address this question, we designed a multiparametric panel allowing the functional study of several thousands of NK cell subsets, and we studied their individual degranulation and IFN-γ secretion upon interaction with different types of tumors.

Materials and Methods

Mice

Wild-type C57BL/6J mice were purchased from Charles River Laboratories. Mice were housed at the animal facility Plateau de Biologie Expérimentale de la Souris, and all experimental studies were performed in accordance with institutional guidelines and approved by the local bioethics committee (Comité d'Éthique en Expérimentation Animale de la Région Rhône-Alpes). Mice at 6–8 wk of age were used.

Single-cell suspensions and flow cytometry

Single-cell suspensions were obtained from harvested spleens. NK cells were purified and stained with fluorophore-conjugated Abs from BD Biosciences, BioLegend, eBioscience, or Miltenyi Biotec against: CD107a (1D4B), CD11b (M1/70), CD27 (LG.7F9), CD3 (145-2C11), CD19 (1D3), DNAM-1 (10E5), KLRG1 (2F1), Ly49A (YE1/48.10.6), Ly49D (4E5), Ly49F (HBF-719), Ly49G2 (4D11), Ly49H (3D10), Ly49I (YLI90), NK1.1 (PK136), NKG2A (20d5), and NKp46 (29A1.4). The mAb 4LO3311 recognizing Ly49C was purified on protein A column from supernatant of the 4LO3311 hybridoma generously provided by Prof. Suzanne Lemieux (Institut Armand Frappier, Laval, QC, Canada). It was detected using a secondary goat anti-IgG3 Ab (SouthernBiotech). NKG2A-positive cells were identified using the 20d5 clone, which also recognizes NKG2C and NKG2E; however, because mouse resting NK cells only express NKG2A, we considered 20d5-reactive cells as NKG2A-positive (33). For intracellular cytokine staining, cells were previously incubated in the presence of 1 μg/ml monensin (BD GolgiStop) for 4 h. Intracellular staining of IFN-γ (XMG1.2) or granzyme B (GzmB; NGZB) was performed with Cytofix/Cytoperm Fixation/Permeabilization Kit (BD Biosciences). Flow cytometry was carried out on a Fortessa 5L (BD Biosciences), fluorescence-minus-one controls were used to set the gates and data analyzed with FlowJo v10 software. The gating strategy is presented in Supplemental Fig. 1.

Generation of RMA-KR cells (MHC-I–deficient and Rae1β-expressing RMA cells)

Single-guide RNAs targeting the first exon of the mouse *B2m* gene (sequence: 5′-AGTCGTCAGCATGGCTCGCT-3′) were cloned into PX458 plasmids also containing the Cas9 gene (Addgene). RMA cells were transfected by electroporation using the Neon transfection system (Thermo Fisher Scientific) with 1 pulse for 50 ms at 1080 V. Cells were sorted by GFP expression 48 h after transfection with an FACSAria II (BD Biosciences). The Rae1β gene was subcloned from Origene plasmid MR220341 into the pRRLSIN-MND-IRES2-ZsGreen-WPRE lentiviral vector (p297). After amplification, MHC-I–deficient RMA cells were transduced with the p297 lentivirus containing Rae1β and incubated for 24 h at a multiplicity of infection of 50. At 48 h after cell transduction, cells were sorted by the expression of ZsGreen.

Cell culture

Both YAC-1 (lymphoma, A/Sn mice) and RMA-KR (lymphoma, C57BL/6J mice) cell lines and splenocytes were cultured in RPMI 1640 medium (Invitrogen Life Technologies) supplemented with 10% FCS, 2 mM L-glutamine, 1% nonessential amino acids (Life Technologies), 1% penicillin/streptomycin (HCL Technologies), 1 mM sodium pyruvate (PAA Laboratories), and 20 mM HEPES (Life Technologies). Adherent cell lines E0771 (mammary tumor, C57BL/6J mice), B16 (melanoma, C57BL/6J mice), and 3T3 (immortalized fibroblasts, Swiss National Institutes of Health mice) were grown in DMEM (Invitrogen Life Technologies) supplemented with 10% FCS and 1% penicillin/streptomycin.

NK cell purification

NK cells were enriched by negative depletion prior to FACS analyses. Splenocyte suspension was incubated with biotinylated Abs from eBioscience or BioLegend against: CD3 (145-2C11), CD5 (53-7.3), CD19 (1D3), Ly6G/Ly6C (RB6-8C5), F4/80 (BM8), CD24 (M1/69), and TER-119 (TER-119), followed by incubation with anti-biotin microbeads (Miltenyi Biotec), and enrichment by magnetic separation on an AutoMACS instrument. Microbeads were used four times less concentrated than recommended to reduce the cost of the experiment and to increase the number of NK cells purified.

NK cell–tumor cocultures

NK cells were first enriched by negative depletion prior to cocultures with tumor cells. Enriched NK cells were cocultured for 4 h with different tumor cell lines at an E:T ratio of 1 in the presence or absence of recombinant murine IL-15 (100 ng/ml; PeproTech). This concentration was previously determined to induce optimal NK cell stimulation (14, 16).

Cell cytotoxicity assay

NK cells purified by negative selection were sorted by flow cytometry according to expression of DNAM-1, NKG2A, and CD27 into triple-positive or triple-negative subsets. Sorted NK cell subsets were plated in 96-well, V-bottom plates and cocultured for 4 h with RMA-KR target cells (MHC-I–deficient and Rae1b-positive) expressing the nanoluciferase (lentivirus-mediated expression) at a concentration of 100 cells/well. Different ratios of NK to target cells were used: 15:1, 5:1, 2:1, and 1:1. After NK cell killing, RMA-KR–derived nanoluciferase was released in the culture supernatant. Nanoluciferase activity in the culture supernatant thus reflects target cell lysis. The total volume in culture wells was 200 μl. Plates were centrifuged briefly for 4 min at 500 × *g*. A total of 50 μl of culture supernatants was collected, and nanoluciferase activity was determined by adding 50 μl of nanoluciferase reagent in black, flat-bottom, 96-well plates. Bioluminescence was measured for 0.1 s with a luminometer (Tecan Group).

Clustering

Clustering analysis of the data sets was performed using unsupervised PhenoGraph and FlowSOM algorithms in R software version 3.5.1 (Cytofkit package, Bioconductor). The number of NK cells was adjusted and samples concatenated, normalized, and plotted on a dimensional reduction *t*-distributed stochastic neighbor embedding (tSNE) visualization. CD107a as well as IFN-γ readouts were excluded from the analysis. Clusters were then reanalyzed in FlowJo software.

Repertoire analysis

NK cell repertoire was determined by automatic Boolean combination gating method in FlowJo software using 12 NK cell receptors as variables, returning 4096 theoretical subpopulations. The Boolean gating function divides cells into all possible receptor combinations measured by using the Boolean operations "and" and "not" on analysis gates applied to those measurements. Cell subpopulations were exported and normalized, and an experiment reproducibility diagnosis was carried out by sample correlation. A threshold of 10 cells in all experimental conditions for every given subpopulation was set to select them for further analysis. Selected subpopulations were sorted by cell abundance and classed into low and high responders by stimulation readout percentages as indicated in text. Heat maps were performed using the Multiple Experiment Viewer software and in R software. Hierarchical clustering with Euclidean distance and optimizing cluster order was applied.

A heat map of receptor's expression was performed based on the logistic regression coefficient matrix, showing how the status of one receptor, represented by "1" or "0," affects the probability of other crossed receptor to be present, also represented by "1" or "0" (i.e., to be existing or missing,

respectively). We calculated P1 as the probability of the outcome receptor existence while the independent receptor exists and P0 as the probability of the outcome receptor existence and the independent receptor does not exist. The odds ratio is calculated as follows: (P1/[1 − P1])/(P0/[1 − P0]).

Differential receptor expression in low and high responder subpopulations for both CD107a and IFN-γ was determined by receptor expression fold change taking into account all experimental replicates.

Statistical analysis

Statistical analyses were performed using GraphPad Prism version 8.2.0. All data sets were tested for normality by Shapiro–Wilk normality test. Pearson correlation was used to compare samples with a normal distribution and Spearman correlation for not normally distributed samples. CD107a or IFN-γ expression between different NK cell subpopulations was compared by paired *t* test when samples were normal and by Wilcoxon matched-pairs signed-rank test when not normal. Differential receptor expression was determined by multiple *t* test without assuming a consistent SD and graphed into a volcano plot. Statistical significance is indicated as follows: $*p < 0.05$, $**p < 0.01$, $***p < 0.001$, $****p < 0.0001$, and $******p < 0.000001$.

Results

Dissection of the NK cell diversity

We sought to investigate the individual antitumor response of murine splenic NK cell subsets defined by the combinatorial expression of multiple NK cell receptors and how the response of each subset was influenced by IL-15 stimulation, which was not previously addressed. We designed a flow cytometry panel (Supplemental Fig. 1A) allowing the simultaneous measurement of 12 membrane receptors, each one expressed only on a fraction of NK cells, which includes NK cell receptors Ly49A, C, D, F, G2, H, I, NKG2A, DNAM-1, and commonly used maturation markers CD11b, CD27, and KLRG1. FITC and PE fluorescence channels were reserved to measure effector functions (CD107a and IFN-γ). NK cells were defined as live lymphocytes with an $NK1.1^+NKp46^+CD3^-$ phenotype (Supplemental Fig. 1B) (34, 35). ILC1 that also have this phenotype were not excluded to limit the number of Abs used, but they represent a minor fraction of $NK1.1^+NKp46^+CD3^-$ cells in the spleen (36), and the questions we asked in this study were also relevant for this cell type. We used a Boolean gating strategy to discriminate positive and negative subsets for each of the 12 markers (Supplemental Fig. 1C), which theoretically resulted in the definition of 4096 combinations or subsets as predicted by the product rule (some combinations are shown in Supplemental Fig. 1D). As many subsets were not present or only contained a few events, we focused our analysis on those ones that included >0.01% of total NK cells (i.e., for which at least 10 NK cells in every experimental condition could be analyzed upon flow cytometry acquisition of 100,000 NK cells). When applying this threshold, only 444 populations were retained that altogether represented >72% of the total NK cell population (Fig. 1A, 1B) and that were remarkably conserved in frequency when comparing different C57BL/6J mice (Fig. 1C). When performing a hierarchical clustering analysis of the different receptors based on their expression in the 444 subsets (Supplemental Fig. 2A), 4 clusters were visible and defined by the coexpression of the following groups of markers: CD27/Ly49A/Ly49G2/Ly49F (cluster 1), CD11b/Ly49H/Ly49D (cluster 2), Ly49C/Ly49I/KLRG1 (cluster 3), and DNAM-1/NKG2ACE (cluster 4). A correlation matrix confirmed the proximity between these receptors and additionally pointed to the anticorrelation between clusters 2/3 and 1 (Supplemental Fig. 2B). Cluster 3 contains the C57BL/6 educating receptors Ly49C and Ly49I and KLRG1, confirming the association between education and KLRG1 expression (37). Cluster 1 contains Ly49A, Ly49G2, and Ly49F that all lack an endogenous MHC ligand in the C57BL/6 background, showing that the expression of these unbound receptors correlates with a lack of educating receptors and maturation markers.

In parallel with Boolean analysis, we wanted to analyze flow cytometry data using an unsupervised method to avoid biases linked to manual gating. For this, we used the Phenograph algorithm, which was previously developed to define subpopulations sharing common phenotypic criteria in complex data sets (38). The Phenograph algorithm identified 16 main clusters (Fig. 1D), and the expression of NK cell receptors across these populations is shown in Fig. 1E. The identified clusters had similar sizes when comparing individual mice (Fig. 1F). The advantage of Phenograph is that it strongly reduces the number of NK cell subsets as compared with the Boolean gating analysis and that it does not exclude any cells from the analysis. The drawback of such analysis is that each of the 16 clusters is obviously not as homogeneous as those defined by Boolean gating (Supplemental Fig. 3A).

Broad tumor reactivity of responder NK cell subsets

Next, we analyzed the response of individual NK cell subsets defined by either Boolean or Phenograph analysis for a given readout (IFN-γ or CD107a) following stimulation with tumor cell lines from three different mouse strains expressing variable MHC-I levels. We used cell lines of different origins and H2 types (i.e., lymphocytic [RMA-KR ($H2^b$) and YAC1 ($H2^k$)], epithelial [E0771 ($H2^b$)], fibroblastic [3T3 ($H2^q$)], or melanocytic [B16 ($H2^b$)]) in the presence or absence of IL-15. RMA-KR cells were obtained by knocking out B2m expression (RMA-KO) and by expressing the strong NKG2D ligand Rae1β in RMA cells by lentiviral transduction (Supplemental Fig. 3B). As shown in Supplemental Fig. 4A and 4B, the different cell lines induced different levels of NK cell response (both IFN-γ and CD107a), from the weakly stimulating B16 cells to the strongly stimulating RMA-KR. When analyzing the individual response of Boolean (Supplemental Fig. 4C) or Phenograph (Supplemental Fig. 4D) subsets, we observed an important heterogeneity between subsets, from weak to strong responders, for every tumor condition. IL-15 boosted the NK cell response and especially IFN-γ, irrespective of the tumor condition (Supplemental Fig. 4A, 4B), but a substantial heterogeneity in the individual response of NK cell subsets remained (Supplemental Fig. 4C, 4D).

We then compared the CD107a or the IFN-γ response of each Boolean NK cell subset between the different tumor conditions. As shown in Fig. 2A and 2B, we observed a very good correlation in the mean response of individual subsets between different tumor conditions (example shown: RMA-KR versus 3T3), with significant *p* values in all comparisons, for both CD107a and IFN-γ. This correlation was even more pronounced when NK cells were stimulated in the presence of IL-15 (Fig. 2C, 2D). To visualize the interexperiment variability, we then expressed as a heat map the individual IFN-γ or CD107a response for each subset and for each tumor type across all experiments with the different tumors with or without IL-15. NK cell subsets were ordered in rows by the mean response in the RMA-KR condition from top to bottom and culture conditions in column by the mean response of all subsets from left to right (Supplemental Fig. 4E). This graph shows a gradient of responses from the top left corner to the bottom right one, both for IFN-γ and CD107a, indicating conservation in the hierarchy of responding subsets across all experiments and tumor conditions.

We also performed a comparison of CD107a or IFN-γ expression by the 16 subsets defined by the Phenograph analysis between the different tumor conditions. As shown in Supplemental Fig. 5A, a similar pattern of response was observed for the 16 subsets for both CD107a and IFN-γ across the different tumor conditions, and this was even more pronounced when NK cells were stimulated in the presence of IL-15. Importantly, IL-15 stimulation did not change the

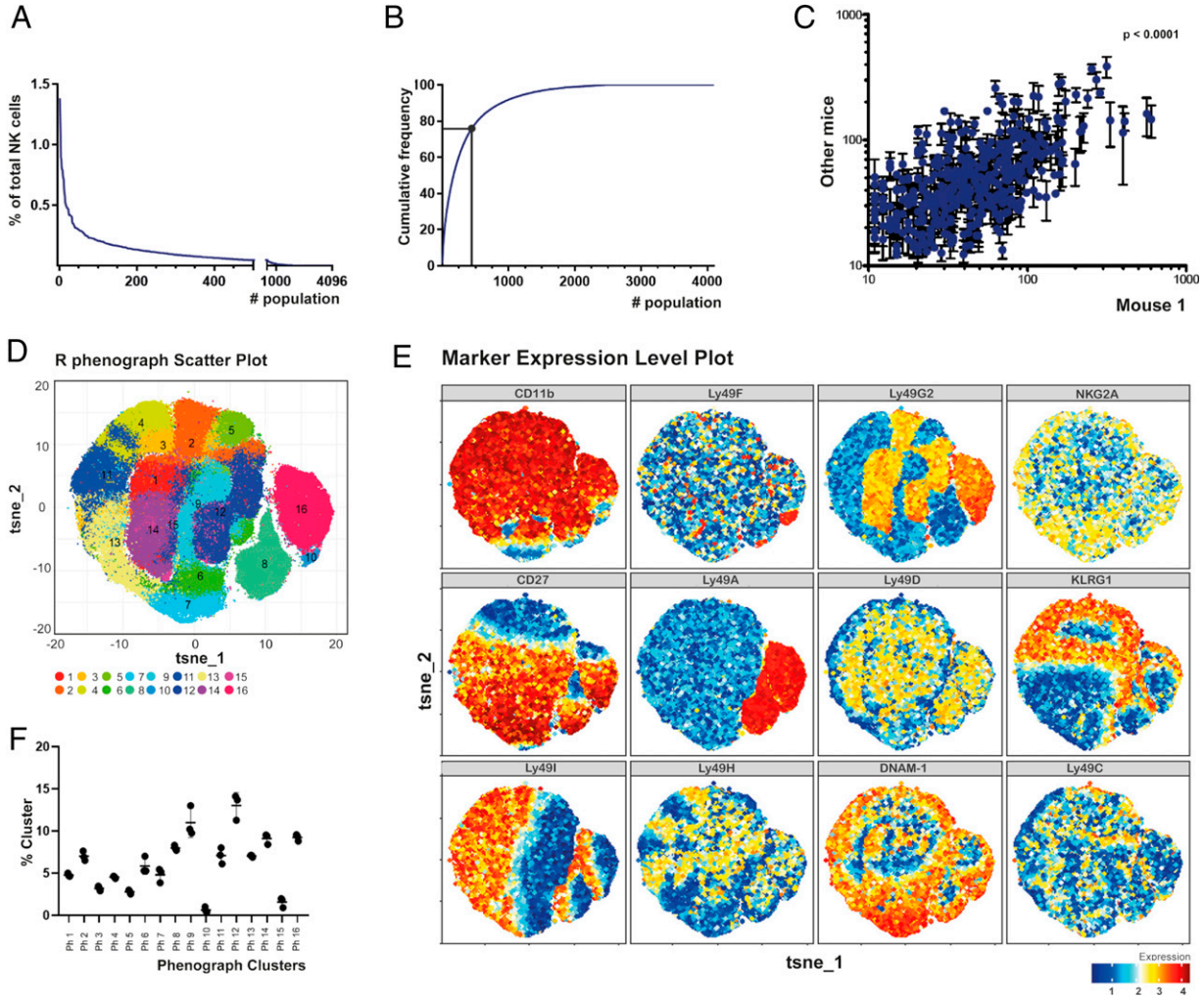

FIGURE 1. Dissection of the NK cell repertoire. (**A**) Splenic NK cell subset percentages defined by Boolean gating strategy in decreasing order. Representative image of seven independent experiments. (**B**) Cumulative frequency of splenic NK cell subsets ordered from highest to lowest percentage. When the threshold of 0.01% of total NK cells is applied, 444 populations are retained as shown in the figure. Representative image of seven independent experiments. (**C**) Correlation of the 444 NK cell subset frequencies defined by Boolean gating strategy between different C57BL/6 mice. Spearman correlation was used to compare one mouse against other three. (**D**) tSNE plot of 16 clusters found by Phenograph algorithm in splenic NK cell population. (**E**) tSNE representation of splenic NK cells colored by receptor expression intensity. (**F**) Percentage of Phenograph NK cell clusters among three different C57BL/6 mice.

pattern of NK cell receptor expression as evaluated by the frequency of the 16 Phenograph clusters in the presence or absence of IL-15 stimulation (Supplemental Fig. 5B).

Altogether, these data suggest that the combinations of NK cell receptors that define NK cell subsets do not encode specificities for different tumor cells but rather different levels of reactivities against tumors, regardless of the tumor type encountered.

Responder NK cell subsets show some degree of specialization at steady state but not after IL-15 priming

Then, we wanted to determine if NK cell subsets defined by Boolean or Phenograph strategies were specialized in IFN-γ secretion versus degranulation. We started by comparing IFN-γ and CD107a expression for all Boolean subsets using the data sets presented in the figures above. As shown in Fig. 3A, there was overall a significant correlation between IFN-γ and CD107a expression in Boolean NK cell subsets in the absence of IL-15. However, in all comparisons, the Spearman R was <0.35, and two groups of populations were visible, with an IFN-γ^{high}CD107a^{low} versus IFN-γ^{low}CD107a^{high} profile, as depicted by the colored ellipses on the graphs in Fig. 3A, suggesting a relative specialization of NK cell subsets for either function. For the Phenograph analysis, we expressed the frequency of IFN-γ– and CD107a-positive NK cells for each cluster as a heat map. This visual analysis showed overall the same specialization that was identified with the Boolean strategy in the absence of IL-15 (Fig. 3C). These data suggest a relative specialization of NK cell subsets for either cytotoxicity or IFN-γ secretion. However, when we performed the same analysis on the data obtained for NK cells stimulated with tumors in the presence of IL-15, a very different picture was obtained, as a good correlation between CD107a and IFN-γ was then observed, for both types of analyses (Boolean and unsupervised) (Fig. 3B, 3D). Thus, IL-15 stimulation coordinates NK cell effector functions in response to tumors.

CD27$^+$NKG2A$^+$DNAM-1$^+$ are the best degranulating NK cells

Next, we wanted to identify which receptor combinations correlated best with NK cell reactivity. To this aim, we defined low responder and high responder subsets for each stimulatory condition on the basis of a graphical representation shown in Supplemental Fig. 6A for the Boolean analysis. For the Phenograph analysis, low responders were defined as the two clusters with the lowest reactivity and high responders were the two clusters with the highest reactivity. We then identified the differentially expressed receptors between both responder groups and plotted the results as a volcano plot

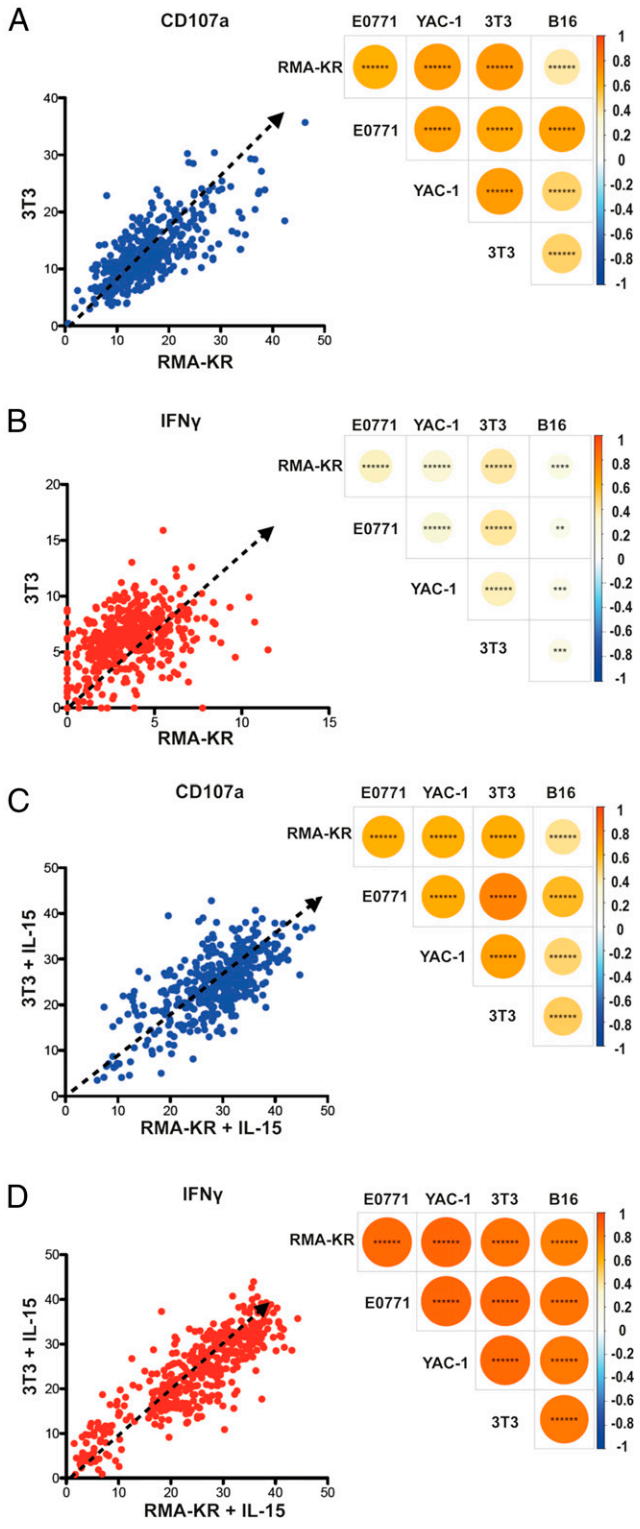

FIGURE 2. Broad tumor reactivity of responder NK cell subsets. Comparison of CD107a (**A** and **C**) or IFN-γ (**B** and **D**) response of Boolean NK cell subsets between different tumor conditions. RMA-KR versus 3T3 comparison is shown as an example. Correlations were performed in absence (A and B) or in presence (C and D) of IL-15. Both circle size and color intensity correspond to the Pearson correlation coefficient. Seven independent experiments were considered for the analysis and Pearson correlation was used as statistical test. $^{**}p < 0.01$, $^{***}p < 0.001$, $^{****}p < 0.0001$, $^{******}p < 0.000001$.

showing fold change and p value, taking into account all tumor conditions.

Degranulation was positively correlated with the expression of the three receptors CD27, DNAM-1, and NKG2A, both for Boolean and Phenograph analysis (Fig. 4A). The analysis of NK cell receptors that negatively correlated with degranulation was less informative, as it was partially discordant between Boolean and Phenograph approaches and the fold change of the differential expression was rather low. A FlowJo analysis confirmed that the triple expression of CD27, DNAM-1, and NKG2A identifies the subset with the highest degranulation potential, irrespective of the tumor used (Fig. 4B). Moreover, this potential was commensurate to the number of receptors expressed, with NKG2A being the most important one. $CD27^+NKG2A^+DNAM1^+$ NK cells are also quite abundant as they represent ~14% of total NK cells in C57BL/6 mice (Fig. 4C).

Even though degranulation and cytotoxicity are usually correlated in NK cells (39, 40), we wanted to confirm our results using a cytotoxicity assay. We sorted spleen NK cells according to CD27, NKG2A, and DNAM-1 expression into triple-negative and triple-positive subsets and compared their capacity to kill RMA-KR cells during a 4-h coculture. As shown in Fig. 4D, $CD27^+NKG2A^+DNAM1^+$ NK cells had indeed a better killer potential than $CD27^-NKG2A^-DNAM1^-$ NK cells. This higher killing potential was also correlated with the levels of GzmB that increased upon coexpression of CD27, NKG2A, and DNAM-1 (Fig. 4E).

$CD11b^+KLRG1^+$ are the best IFN-γ–secreting NK cells

For IFN-γ, both Boolean and Phenograph analyses returned a positive correlation with the maturation markers KLRG1 and CD11b and, to a lesser extent, with education receptors Ly49I, Ly49C, and NKG2A (Fig. 5A). Both analyses also showed a negative correlation with the unbound receptors Ly49A, Ly49F, and Ly49G2 and CD27. To confirm these results, we used FlowJo to analyze how the combination of these different receptors impacted IFN-γ production and NK cell frequency. Results in Fig. 5B show that CD11b and KLRG1 were sufficient to define good IFN-γ producers. This was due overall to a very low frequency of cells expressing the receptors with a negative impact (i.e., CD27, Ly49A, Ly49F, and Ly49G2) in the $CD11b^+KLRG1^+$ subset. Moreover, $CD11b^+KLRG1^+$ NK cells were, for the majority, educated cells expressing one or more educating receptors (Fig. 5C). The lack of CD11b and KLRG1 was, however, not sufficient to define weak IFN-γ producers, and combining the expression of CD27 and especially Ly49A and Ly49G2 was important to define the lowest IFN-γ–expressing cells (Fig. 5B) (Ly49F was also involved but in a minority of subsets). This suggests a major impact of unbound inhibitory receptors on IFN-γ secretion capacity. To explore further this effect, we compared the IFN-γ secretion capacity of $CD11b^+KLRG1^+CD27^-$ NK cells expressing zero, one, or two unbound receptors. Results in Fig. 5D show that unbound receptors have a negative correlation with IFN-γ expression, again commensurate to the numbers of receptors expressed. This suggests that those receptors prevent the positive effects of maturation and education on reactivity.

IL-15 coordinates NK cell functions, and $CD11b^+KLRG1^+$ NK cells are the best effectors

Finally, we correlated receptor expression and effector functions when NK cells were stimulated with tumors in the presence of IL-15. As shown in Fig. 6, the correlation volcano plots gave a different picture than in the absence of IL-15. Indeed, this analysis shows that maturation as defined by CD11b/KLRG1 was the main driver of NK cell reactivity with a lesser impact of all other receptors, both for CD107 and IFN-γ effector responses, irrespective of the type of analysis (i.e., Boolean and Phenograph algorithm). There was also a negative correlation with unbound receptors, especially for IFN-γ (Fig. 6). A FlowJo analysis confirmed that the lack of KLRG1 and especially

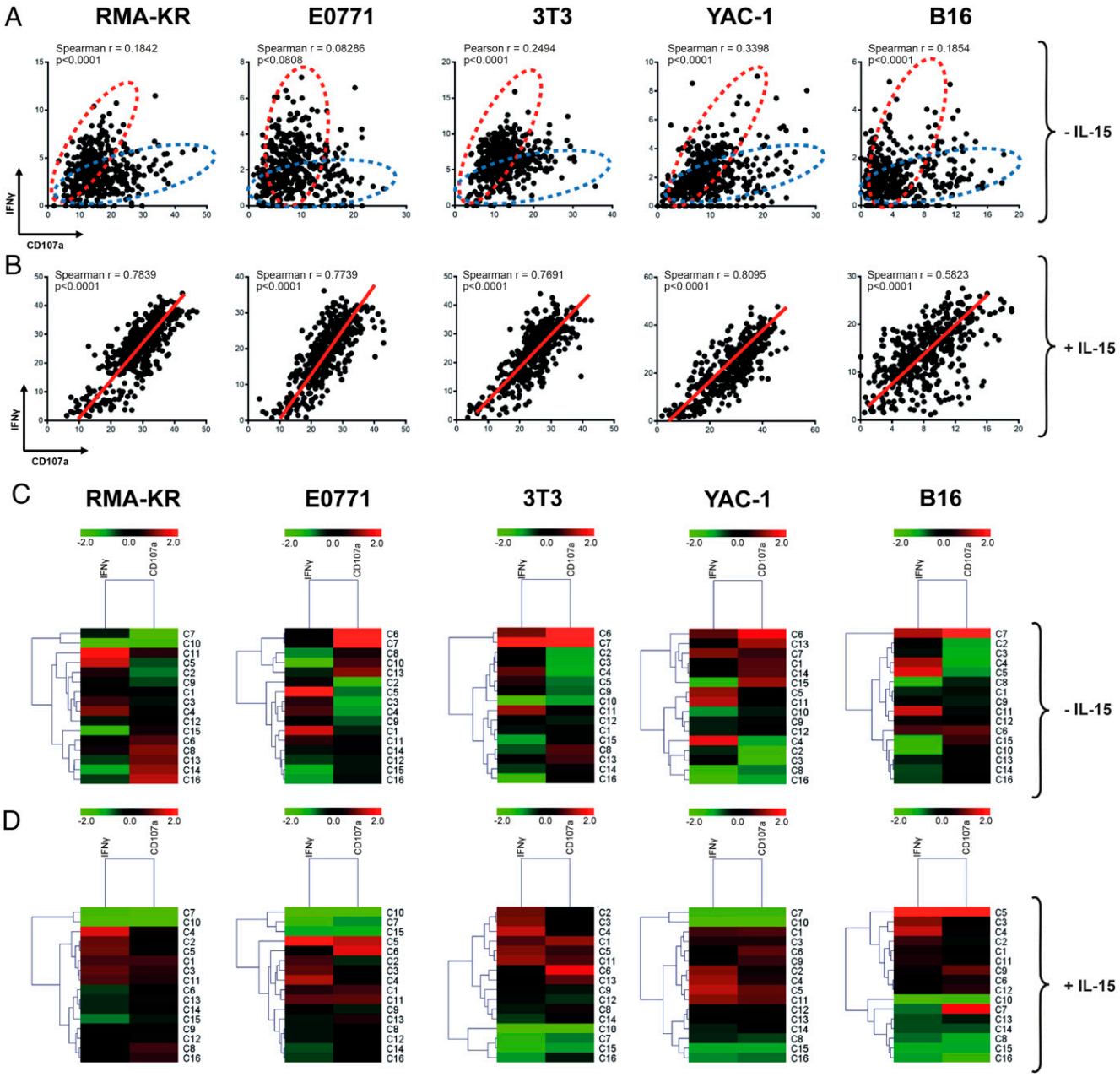

FIGURE 3. Responder NK cell subsets show some degree of specialization at steady state but not after IL-15 priming. Correlation between CD107a and IFN-γ expression in Boolean NK cell subsets across different stimulation conditions without (**A**) and in presence (**B**) of IL-15. Spearman or Pearson correlation was used as indicated on the graphs, and results from seven independent experiments were considered for the analysis. Hierarchical clustering based on Euclidean distance of normalized Phenograph NK cell clusters determined by CD107a and IFN-γ expression across different stimulation conditions without (**C**) and in presence (**D**) of IL-15. One representative experiment out of seven is shown.

CD11b defined the less reactive NK cells both in terms of degranulation and IFN-γ production and that unbound receptors retained a negative effect even on $CD11b^-$ cells, especially for IFN-γ production (Supplemental Fig. 6B, 6C).

Thus, IL-15 coordinates NK cell functions, and $CD11b^+KLRG1^+$ NK cells are the best responder cells when NK cells are stimulated in the presence of IL-15.

Discussion

The NK cell repertoire is generated by the combinatorial expression of NK cell activating and inhibitory receptors. A previous study that analyzed human NK cell receptors expression using mass cytometry uncovered a large complexity of this repertoire with tens of thousands of subsets (21). However, the functional potential of these subsets was not investigated. In this study, we addressed this question using flow cytometry and a more restricted Ab panel that include many of the main variegated NK cell receptors. For some of the receptors (e.g., Ly49I), the separation between positive and negative cells was not as optimal as for other receptors (e.g., Ly49A, Ly49G2, etc.), which could result from a lower expression level of the corresponding receptors and/or from a weaker brightness of some fluorochromes. However, these technical hurdles of the FACS technology cannot be avoided when using many Abs simultaneously. We used both supervised and unsupervised methods to analyze flow cytometry data. The supervised analysis consists in a Boolean gating procedure that considers all possible subsets. Many of the 4096 populations that we defined were, however, very small,

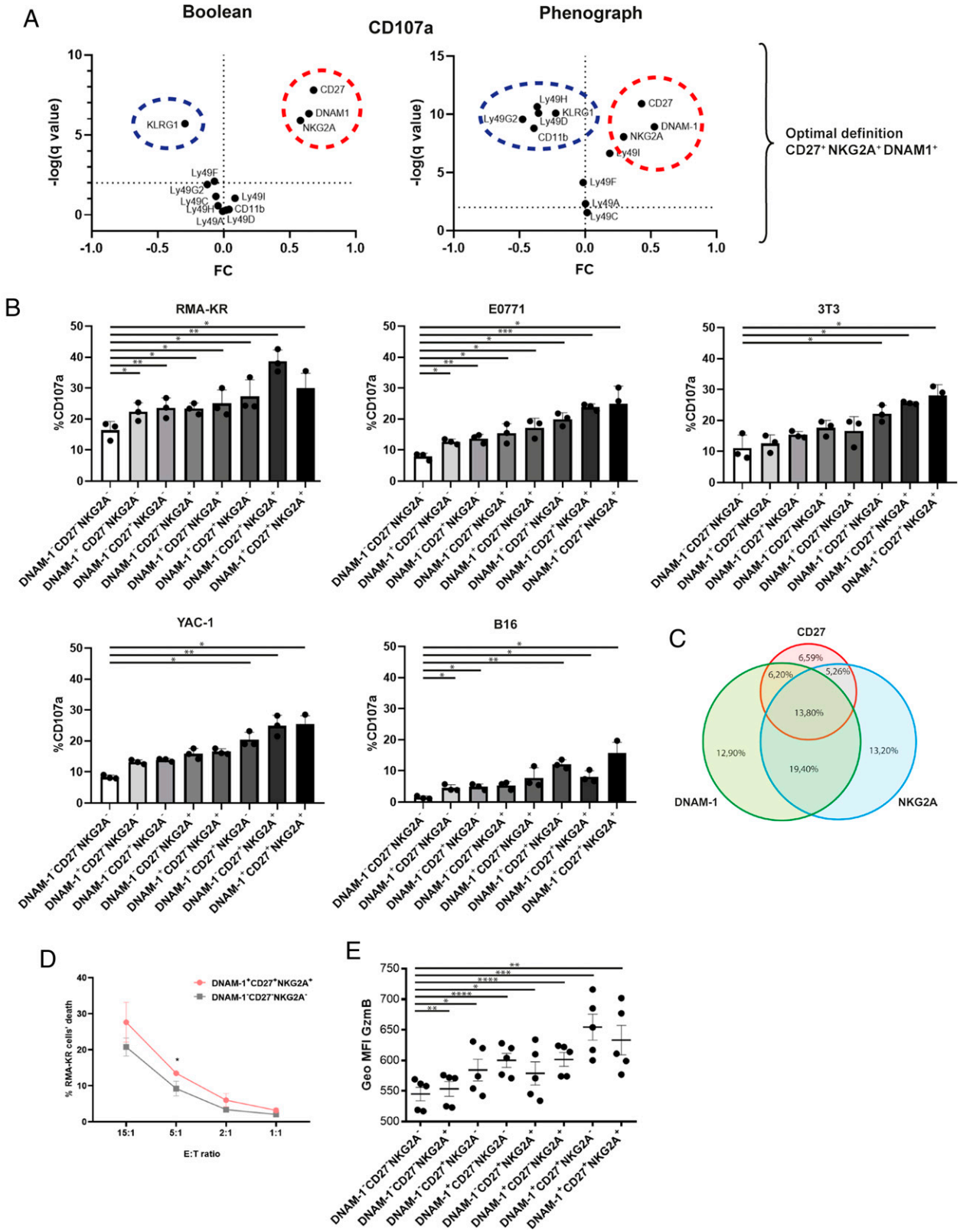

FIGURE 4. $CD27^{+}NKG2A^{+}DNAM\text{-}1^{+}$ are the best degranulating NK cells. (**A**) Volcano plots of receptor expression fold change (FC) between high and low responder NK cell subsets for CD107a expression. This analysis was performed by multiple *t* tests for NK cell subsets determined by Boolean gating (left) and clusters determined by Phenograph strategy (right). Seven and one representative experiment shown, respectively. Red circles highlight positive receptor correlation with response, and blue circles negative receptor correlation. (**B**) Mean percentage of CD107a expression in subgated NK cell populations according to the combinatorial expression of DNAM-1, CD27, and NKG2A receptors for the five tumor-stimulating conditions in three independent experiments. Comparisons were performed by paired *t* tests. Only significant differences with the $DNAM\text{-}1^{-}CD27^{-}NKG2A^{-}$ subset are shown in the graphs. (**C**) Mean relative abundance of each NK cell subset determined by combinatorial expression of DNAM-1, CD27, and NKG2A receptors. (**D**) Cytotoxicity assay of sorted NK cell subsets, as defined in the figure, against RMA-KR cells. Results show the mean ± SD results of three individual mice. Comparisons were performed using paired *t* tests. (**E**) Geometric mean fluorescence intensity (Geo MFI) of GzmB staining in the indicated NK cell subsets, as measured by flow cytometry; $n = 5$. Comparisons were performed using paired *t* tests. $^{*}p < 0.05$, $^{**}p < 0.01$, $^{***}p < 0.001$, $^{****}p < 0.0001$.

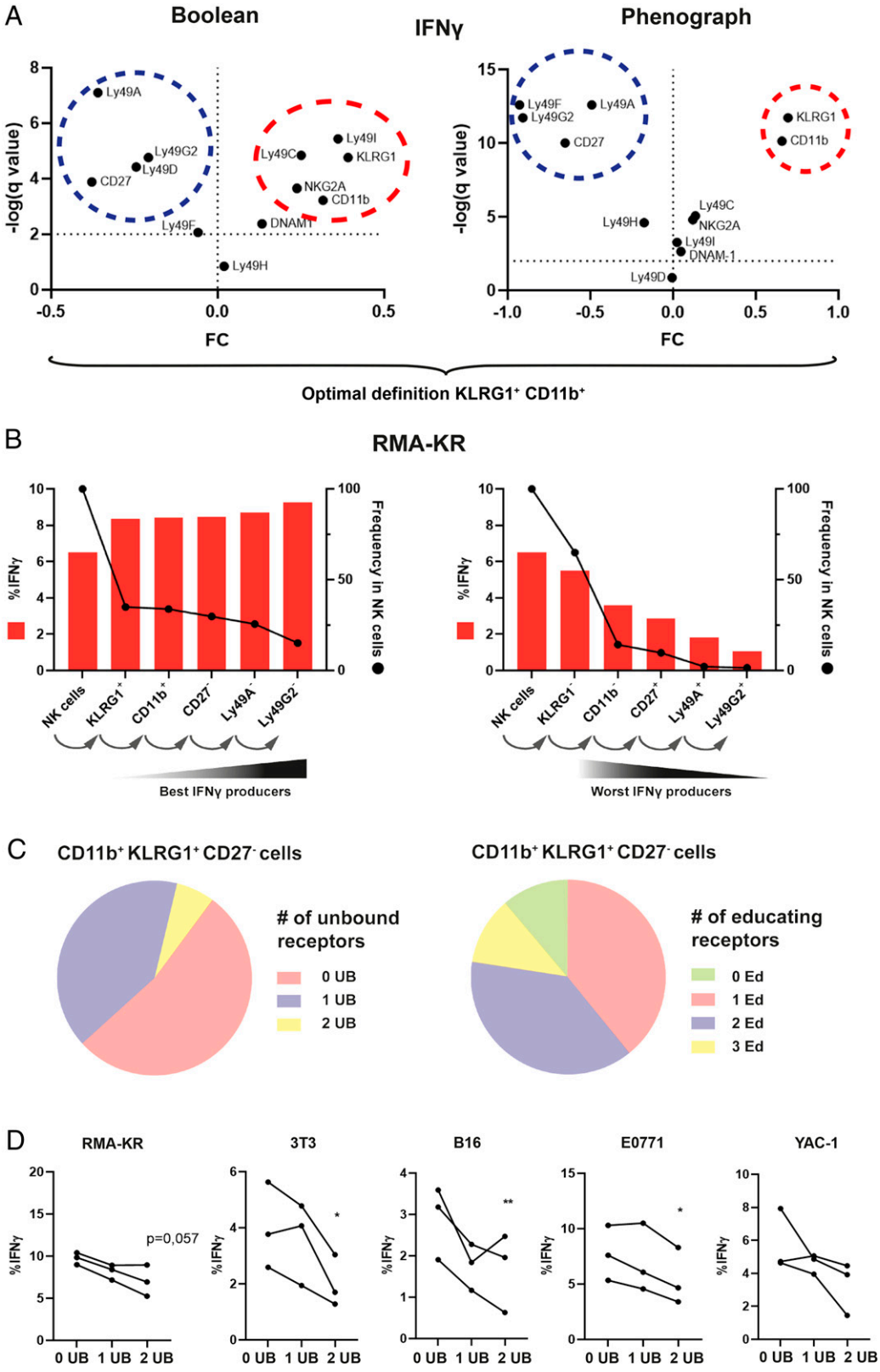

FIGURE 5. $CD11b^{+}KLRG1^{+}$ are the best IFN-γ–secreting cells. (**A**) Volcano plots of receptor expression fold change (FC) between high and low responder NK cell subsets for IFN-γ expression. This analysis was performed by multiple *t* tests for NK cell subsets determined by Boolean gating (left) and clusters determined by Phenograph strategy (right). Red circles highlight positive receptor correlation with response, and blue circles negative receptor correlation. (**B**) IFN-γ expression against RMA-KR cell line across sequential gating by KLRG1, CD11b, CD27, Ly49A, and Ly49G2 receptor expression defining the best (left) and the worst (right) IFN-γ producers. The bars represent percentage of IFN-γ, and the black dots and connecting line represent the frequency of the NK cell subset among all NK cells. One representative experiment out of seven is shown. (**C**) Frequency of $CD11b^{+}KLRG1^{+}CD27^{-}$ NK cell subsets expressing 0, 1, or 2 unbound (UB) receptors (left) or 0, 1, 2, or 3 educating (Ed) receptors (right). (**D**) IFN-γ percentage in $CD11b^{+}CD27^{-}KLRG1^{+}$ NK cells expressing 0, 1, or 2 UB receptors across different tumor stimulation conditions. Comparisons were performed by paired *t* tests. $*p < 0.05$, $**p < 0.01$.

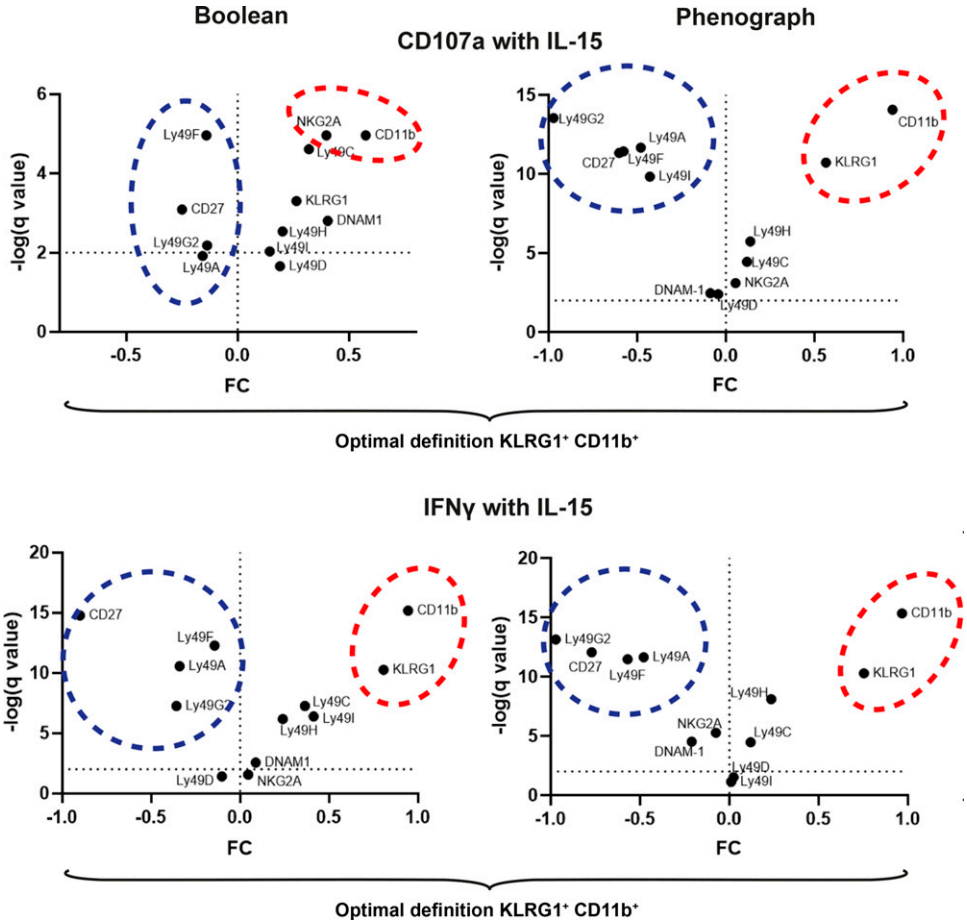

FIGURE 6. CD11b$^+$KLRG1$^+$ are the best degranulating and IFN-γ–secreting subsets in the presence of IL-15. Volcano plots of receptor expression fold change (FC) between high and low responder NK cell subsets for CD107a (top) and IFN-γ (bottom) expression. This analysis was performed by multiple *t* tests for NK cell subsets determined by Boolean gating (left) and clusters determined by Phenograph strategy (right). Red circles highlight positive receptor correlation with response and blue circles negative receptor correlation.

at the limit of what we could analyze with good confidence, which explains why we focused on the 444 most abundant ones. The lower threshold that we used to select these subsets (at least 10 cells acquired in every experimental condition) remained quite low, but cell subsets defined this way have a well-conserved frequency between different mice. Moreover, we obtained similar results when applying higher thresholds. The unsupervised Phenograph analysis that we used has the advantage of being exhaustive, but the reduction of complexity that it implies (identifying 16 clusters in this case) may suppress some of the complexity we were interested in. Thus, both strategies have intrinsic but different limitations, and we therefore used both of them to analyze NK cell diversity.

What is the purpose of NK cell diversity? Previous studies have shown a surprising capacity of NK cells to react against different chemicals (41) or protein peptides (42) and, even more surprisingly, to discriminate between them in experimental settings of contact-hypersensitivity reactions. Human memory NK cells specific for viral Ags were also observed in vaccinated individuals in a recent report (43). The concept of Ag-specific memory NK cells implies that NK cells express surface structures capable of discriminating different Ags. Speculations about RAG-independent gene rearrangements underlying this recognition were not substantiated by direct evidence (44), thus suggesting that Ag specificity is held by NK cell receptor combinations. We address this question in the context of antitumor responses using a variety of tumor cell lines. We found that the best responding NK cell populations were similar for each of the tumor conditions we used, and overall, we observed a very good and statistically significant conservation in the hierarchy of NK cell subsets responding against different tumor types. This was unexpected because the tumors we used had very different tissue origins, suggesting they expressed distinct sets of ligands for activating and inhibitory ligands. The general mechanisms of tumor cell recognition by NK cells are thought to be similar for tumors of hematopoietic versus nonhematopoietic origin (30, 45), yet the receptors and the NK cell subsets involved could be different as signaling lymphocytic activation molecule family receptors may be more adapted to the recognition of hematopoietic malignancies (46), whereas KLRG1 and CRTAM may rather contribute to the recognition of tumors of epithelial origin (47). Thus, we conclude that NK cell receptor combinations do not encode for different tumor specificities but rather for different levels of reactivity. Further studies should be considered to confirm these results in in vivo tumor models. Moreover, even though our combinatorial analysis included 12 receptors, we cannot exclude that other receptors not included in our Ab panel could drive some tumor-specific responses.

We observed some level of effector specialization, at least when stimulation experiments were performed in the absence of exogenous cytokines (i.e., IL-15). The coexpression of DNAM-1, CD27, and NKG2A was associated with the capacity of NK cells to kill tumor cells, as measured by CD107a exposure and cytotoxicity assay. All three receptors were previously associated with better NK cell reactivity against various tumors when assessed individually (5, 48, 49). However, our study is the first one, to our knowledge, to show that the combined expression of all three receptors defines the best NK cell responder populations in terms of degranulation. NKG2A and especially CD27 are not expressed in terminally differentiated NK cells (5, 6), thus showing that the best killer capacity is acquired before terminal differentiation. DNAM-1 expression has been associated with a more active IL-15R pathway (48), and our own studies previously showed the importance of the mTOR

pathway downstream IL-15R in the control of the cytotoxic machinery (11, 16). Moreover, human NKG2A$^+$CD57$^-$ NK cells were recently shown to proliferate more and to activate the mTOR complex 1 at higher levels than NKG2A$^-$CD57$^+$ NK cells (50). Thus, DNAM-1/NKG2A coexpression may lead to optimal mTOR activation. In humans, DNAM-1 expression has been shown to correlate with NK cell education (51). Although we do not confirm this point in mouse NK cells (no correlation between educating receptors and DNAM-1), NKG2A-mediated education may be sufficient to combine with DNAM-1 to trigger NK cell adhesion to tumors and cytotoxicity. Moreover, DNAM-1 was previously shown to synergize with other activating receptors for resting NK cell activation upon cross-linking with Abs (52). DNAM-1 is known to signal via a conserved tyrosine- and asparagine-based motif in the cytoplasmic domain. Upon phosphorylation by Src kinases, this motif enables binding of DNAM-1 to adaptor Grb2, leading to activation of enzymes Vav-1, PI3K, and phospholipase Cγ1, and promotes activation of Erk and Akt kinases and calcium flux (53). CD27 is a classical costimulatory molecule (54) expressed by multiple lymphocyte subsets. It binds to CD70, which leads to NF-κB activation (55), and promotes T cell survival (56). Although in-depth studies are needed to address the mechanism by which CD27$^+$NKG2A$^+$DNAM-1$^+$ degranulate better toward tumor cells, one can hypothesize that this subset may be metabolically more active and that CD27 and DNAM-1 signaling pathways may synergize to induce NK cell cytotoxicity.

We observed that IFN-γ secretion in response to stimulation by tumor cells was more efficiently induced in mature CD11b$^+$KLRG1$^+$ NK cells. This phenotype correlates somehow with the expression of educating receptors Ly49C and Ly49I but is not completely overlapping, thus showing that functional calibration of NK cells is a complex phenomenon based on noncoordinated mechanisms like cell differentiation and education, as previously discussed (19). A previous study also showed that combined expression of educating receptors correlated well with the capacity of NK cells to produce IFN-γ in response to YAC-1 cells stimulation but less well with the degranulating capacity (57). Mice lacking Ly49-mediated NK licensing display reduced antitumor responses in different models, such as methylcholanthrene-induced sarcoma and spontaneous B cell lymphoma (58). KLRG1 expression is known to be controlled by T-bet in NK cells (37), and this transcription factor is also known to be more expressed by terminally mature KLRG1$^+$ NK cells (36) and an important epigenetic regulator of IFN-γ expression (59). Moreover, T-bet–deficient mice injected i.v. with syngeneic melanoma or colorectal carcinoma cells are more susceptible to metastatic spreading than control mice, which can be prevented by adoptive transfer of purified CD27$^-$KLRG1$^+$ NK cells (60, 61). Thus, T-bet–dependent KLRG1$^+$ NK cells may be particularly important to eliminate metastatic cells via the production of IFN-γ. Interestingly, we found a negative impact of unbound inhibitory receptors on the capacity of NK cells to produce IFN-γ in response to tumor stimulation, and these receptors could even overcome the positive effect of educated receptors, a phenomenon also observed in a previous study that did not include as many receptors as the present one (7). As education is known to be dependent on SHP-1 (10), one could consider a competition for limited levels of SHP-1 between inhibitory receptors, regardless of the presence of their ligands in NK cell environment. This model is supported by the previous observation that a dominant-negative form of SHP-1 competing with endogenous SHP-1 reduced NK cell reactivity in a transgenic mouse model (62).

It has long been known that IL-15 stimulation boosts NK cell reactivity (13). However, whether IL-15 homogeneously affects all NK cell subsets is not well understood. Previous studies have shown that educated NK cells (63) or DNAM-1–expressing cells (48) responded better to IL-15 in terms of survival or proliferation, respectively, but how other receptors influence this reactivity is unknown. We observed that IL-15 stimulation coordinated NK cell responses (i.e., degranulation and IFN-γ secretion against tumors). This effect was particularly important for populations that were not very reactive in the absence of IL-15. Previous articles also showed that hyporesponsive uneducated NK cells could be rendered reactive by in vitro cytokine priming (11) or by in vivo stimulation with TLR ligands (58), which induces high IL-15 expression (17). IL-15 is known to boost NK cell cytotoxic function (64, 65), in part through the upregulation of mTOR activity and associated metabolism (16, 66). Moreover, IL-15 and other proinflammatory cytokines can boost T-bet expression in NK cells (15) to amplify their capacity to produce IFN-γ. Thus, IL-15 may amplify different signaling circuits to coordinate and optimize antitumor effector functions of multiple NK cell subsets, largely overcoming differences in reactivities regulated by NK cell receptors.

Acknowledgments

We thank the SFR Biosciences (UMS3444/CNRS, ENSL, UCBL, US8/INSERM) facilities, in particular the Plateau de Biologie Expérimentale de la Souris, and the flow cytometry facility.

Disclosures

The authors have no financial conflicts of interest.

References

1. Smyth, M. J., Y. Hayakawa, K. Takeda, and H. Yagita. 2002. New aspects of natural-killer-cell surveillance and therapy of cancer. *Nat. Rev. Cancer* 2: 850–861.
2. Vivier, E., E. Tomasello, M. Baratin, T. Walzer, and S. Ugolini. 2008. Functions of natural killer cells. *Nat. Immunol.* 9: 503–510.
3. Raulet, D. H., and N. Guerra. 2009. Oncogenic stress sensed by the immune system: role of natural killer cell receptors. *Nat. Rev. Immunol.* 9: 568–580.
4. Kim, S., K. Iizuka, H.-S. P. Kang, A. Dokun, A. R. French, S. Greco, and W. M. Yokoyama. 2002. In vivo developmental stages in murine natural killer cell maturation. *Nat. Immunol.* 3: 523–528.
5. Hayakawa, Y., and M. J. Smyth. 2006. CD27 dissects mature NK cells into two subsets with distinct responsiveness and migratory capacity. *J. Immunol.* 176: 1517–1524.
6. Chiossone, L., J. Chaix, N. Fuseri, C. Roth, E. Vivier, and T. Walzer. 2009. Maturation of mouse NK cells is a 4-stage developmental program. *Blood* 113: 5488–5496.
7. Guia, S., B. N. Jaeger, S. Piatek, S. Mailfert, T. Trombik, A. Fenis, N. Chevrier, T. Walzer, Y. M. Kerdiles, D. Marguet, et al. 2011. Confinement of activating receptors at the plasma membrane controls natural killer cell tolerance. *Sci. Signal.* 4: ra21.
8. Orr, M. T., and L. L. Lanier. 2010. Natural killer cell education and tolerance. *Cell* 142: 847–856.
9. Bern, M. D., D. L. Beckman, T. Ebihara, S. M. Taffner, J. Poursine-Laurent, J. M. White, and W. M. Yokoyama. 2017. Immunoreceptor tyrosine-based inhibitory motif-dependent functions of an MHC class I-specific NK cell receptor. *Proc. Natl. Acad. Sci. USA* 114: E8440–E8447.
10. Viant, C., A. Fenis, G. Chicanne, B. Payrastre, S. Ugolini, and E. Vivier. 2014. SHP-1-mediated inhibitory signals promote responsiveness and anti-tumour functions of natural killer cells. *Nat. Commun.* 5: 5108.
11. Marçais, A., M. Marotel, S. Degouve, A. Koenig, S. Fauteux-Daniel, A. Drouillard, H. Schlums, S. Viel, L. Besson, O. Allatif, et al. 2017. High mTOR activity is a hallmark of reactive natural killer cells and amplifies early signaling through activating receptors. *eLife* 6: e26423.
12. Goodridge, J. P., B. Jacobs, M. L. Saetersmoen, D. Clement, Q. Hammer, T. Clancy, E. Skarpen, A. Brech, J. Landskron, C. Grimm, et al. 2019. Remodeling of secretory lysosomes during education tunes functional potential in NK cells. *Nat. Commun.* 10: 514.
13. Marçais, A., S. Viel, M. Grau, T. Henry, J. Marvel, and T. Walzer. 2013. Regulation of mouse NK cell development and function by cytokines. *Front. Immunol.* 4: 450.
14. Viel, S., A. Marçais, F. S.-F. Guimaraes, R. Loftus, J. Rabilloud, M. Grau, S. Degouve, S. Djebali, A. Sanlaville, E. Charrier, et al. 2016. TGF-β inhibits the activation and functions of NK cells by repressing the mTOR pathway. *Sci. Signal.* 9: ra19.
15. Yu, J., M. Wei, B. Becknell, R. Trotta, S. Liu, Z. Boyd, M. S. Jaung, B. W. Blaser, J. Sun, D. M. Benson, Jr., et al. 2006. Pro- and antiinflammatory cytokine signaling: reciprocal antagonism regulates interferon-gamma production by human natural killer cells. *Immunity* 24: 575–590.

16. Marçais, A., J. Cherfils-Vicini, C. Viant, S. Degouve, S. Viel, A. Fenis, J. Rabilloud, K. Mayol, A. Tavares, J. Bienvenu, et al. 2014. The metabolic checkpoint kinase mTOR is essential for IL-15 signaling during the development and activation of NK cells. *Nat. Immunol.* 15: 749–757.
17. Lucas, M., W. Schachterle, K. Oberle, P. Aichele, and A. Diefenbach. 2007. Dendritic cells prime natural killer cells by trans-presenting interleukin 15. *Immunity* 26: 503–517.
18. Urlaub, D., K. Höfer, M.-L. Müller, and C. Watzl. 2017. LFA-1 activation in NK cells and their subsets: influence of receptors, maturation, and cytokine stimulation. *J. Immunol.* 198: 1944–1951.
19. Goodridge, J. P., B. Önfelt, and K.-J. Malmberg. 2015. Newtonian cell interactions shape natural killer cell education. *Immunol. Rev.* 267: 197–213.
20. Kadri, N., A. K. Wagner, S. Ganesan, K. Kärre, S. Wickström, M. H. Johansson, and P. Höglund. 2016. Dynamic regulation of NK cell responsiveness. *Curr. Top. Microbiol. Immunol.* 395: 95–114.
21. Horowitz, A., D. M. Strauss-Albee, M. Leipold, J. Kubo, N. Nemat-Gorgani, O. C. Dogan, C. L. Dekker, S. Mackey, H. Maecker, G. E. Swan, et al. 2013. Genetic and environmental determinants of human NK cell diversity revealed by mass cytometry. *Sci. Transl. Med.* 5: 208ra145.
22. Arstila, T. P., A. Casrouge, V. Baron, J. Even, J. Kanellopoulos, and P. Kourilsky. 1999. A direct estimate of the human alphabeta T cell receptor diversity. *Science* 286: 958–961.
23. Held, W., J. D. Coudert, and J. Zimmer. 2003. The NK cell receptor repertoire: formation, adaptation and exploitation. *Curr. Opin. Immunol.* 15: 233–237.
24. Vivier, E., D. H. Raulet, A. Moretta, M. A. Caligiuri, L. Zitvogel, L. L. Lanier, W. M. Yokoyama, and S. Ugolini. 2011. Innate or adaptive immunity? The example of natural killer cells. *Science* 331: 44–49.
25. Hammer, Q., T. Rückert, E. M. Borst, J. Dunst, A. Haubner, P. Durek, F. Heinrich, G. Gasparoni, M. Babic, A. Tomic, et al. 2018. Peptide-specific recognition of human cytomegalovirus strains controls adaptive natural killer cells. *Nat. Immunol.* 19: 453–463.
26. Hammer, Q., T. Rückert, and C. Romagnani. 2018. Natural killer cell specificity for viral infections. *Nat. Immunol.* 19: 800–808.
27. Arase, H., E. S. Mocarski, A. E. Campbell, A. B. Hill, and L. L. Lanier. 2002. Direct recognition of cytomegalovirus by activating and inhibitory NK cell receptors. *Science* 296: 1323–1326.
28. Smith, H. R. C., J. W. Heusel, I. K. Mehta, S. Kim, B. G. Dorner, O. V. Naidenko, K. Iizuka, H. Furukawa, D. L. Beckman, J. T. Pingel, et al. 2002. Recognition of a virus-encoded ligand by a natural killer cell activation receptor. *Proc. Natl. Acad. Sci. USA* 99: 8826–8831.
29. Béziat, V., L. L. Liu, J.-A. Malmberg, M. A. Ivarsson, E. Sohlberg, A. T. Björklund, C. Retière, E. Sverremark-Ekström, J. Traherne, P. Ljungman, et al. 2013. NK cell responses to cytomegalovirus infection lead to stable imprints in the human KIR repertoire and involve activating KIRs. *Blood* 121: 2678–2688.
30. Desbois, M., S. Rusakiewicz, C. Locher, L. Zitvogel, and N. Chaput. 2012. Natural killer cells in non-hematopoietic malignancies. *Front. Immunol.* 3: 395.
31. Dhar, P., and J. D. Wu. 2018. NKG2D and its ligands in cancer. *Curr. Opin. Immunol.* 51: 55–61.
32. Barrow, A. D., and M. Colonna. 2019. Exploiting NK cell surveillance pathways for cancer therapy. *Cancers (Basel)* 11: 55.
33. Vance, R. E., J. R. Kraft, J. D. Altman, P. E. Jensen, and D. H. Raulet. 1998. Mouse CD94/NKG2A is a natural killer cell receptor for the nonclassical major histocompatibility complex (MHC) class I molecule Qa-1(b). *J. Exp. Med.* 188: 1841–1848.
34. Robinette, M. L., A. Fuchs, V. S. Cortez, J. S. Lee, Y. Wang, S. K. Durum, S. Gilfillan, and M. Colonna; Immunological Genome Consortium. 2015. Transcriptional programs define molecular characteristics of innate lymphoid cell classes and subsets. *Nat. Immunol.* 16: 306–317.
35. Branzk, N., K. Gronke, and A. Diefenbach. 2018. Innate lymphoid cells, mediators of tissue homeostasis, adaptation and disease tolerance. *Immunol. Rev.* 286: 86–101.
36. Daussy, C., F. Faure, K. Mayol, S. Viel, G. Gasteiger, E. Charrier, J. Bienvenu, T. Henry, E. Debien, U. A. Hasan, et al. 2014. T-bet and Eomes instruct the development of two distinct natural killer cell lineages in the liver and in the bone marrow. *J. Exp. Med.* 211: 563–577.
37. Robbins, S. H., M. S. Tessmer, L. Van Kaer, and L. Brossay. 2005. Direct effects of T-bet and MHC class I expression, but not STAT1, on peripheral NK cell maturation. *Eur. J. Immunol.* 35: 757–765.
38. Levine, J. H., E. F. Simonds, S. C. Bendall, K. L. Davis, A. D. Amir, M. D. Tadmor, O. Litvin, H. G. Fienberg, A. Jager, E. R. Zunder, et al. 2015. Data-driven phenotypic dissection of AML reveals progenitor-like cells that correlate with prognosis. *Cell* 162: 184–197.
39. Alter, G., J. M. Malenfant, and M. Altfeld. 2004. CD107a as a functional marker for the identification of natural killer cell activity. *J. Immunol. Methods* 294: 15–22.
40. Aktas, E., U. C. Kucuksezer, S. Bilgic, G. Erten, and G. Deniz. 2009. Relationship between CD107a expression and cytotoxic activity. *Cell. Immunol.* 254: 149–154.
41. O'Leary, J. G., M. Goodarzi, D. L. Drayton, and U. H. von Andrian. 2006. T cell- and B cell-independent adaptive immunity mediated by natural killer cells. *Nat. Immunol.* 7: 507–516.
42. Paust, S., H. S. Gill, B.-Z. Wang, M. P. Flynn, E. A. Moseman, B. Senman, M. Szczepanik, A. Telenti, P. W. Askenase, R. W. Compans, and U. H. von Andrian. 2010. Critical role for the chemokine receptor CXCR6 in NK cell-mediated antigen-specific memory of haptens and viruses. *Nat. Immunol.* 11: 1127–1135.
43. Nikzad, R., L. S. Angelo, K. Aviles-Padilla, D. T. Le, V. K. Singh, L. Bimler, M. Vukmanovic-Stejic, E. Vendrame, T. Ranganath, L. Simpson, et al. 2019. Human natural killer cells mediate adaptive immunity to viral antigens. *Sci. Immunol.* 4: eaat8116.
44. Paust, S., C. A. Blish, and R. K. Reeves. 2017. Redefining memory: building the case for adaptive NK cells. *J. Virol.* 91: e00169-17.
45. Viel, S., E. Charrier, A. Marçais, P. Rouzaire, J. Bienvenu, L. Karlin, G. Salles, and T. Walzer. 2013. Monitoring NK cell activity in patients with hematological malignancies. *OncoImmunology* 2: e26011.
46. Wu, N., M.-C. Zhong, R. Roncagalli, L.-A. Pérez-Quintero, H. Guo, Z. Zhang, C. Lenoir, Z. Dong, S. Latour, and A. Veillette. 2016. A hematopoietic cell-driven mechanism involving SLAMF6 receptor, SAP adaptors and SHP-1 phosphatase regulates NK cell education. *Nat. Immunol.* 17: 387–396.
47. Chockley, P. J., J. Chen, G. Chen, D. G. Beer, T. J. Standiford, and V. G. Keshamouni. 2018. Epithelial-mesenchymal transition leads to NK cell-mediated metastasis-specific immunosurveillance in lung cancer. *J. Clin. Invest.* 128: 1384–1396.
48. Martinet, L., L. Ferrari De Andrade, C. Guillerey, J. S. Lee, J. Liu, F. Souza-Fonseca-Guimaraes, D. S. Hutchinson, T. B. Kolesnik, S. E. Nicholson, N. D. Huntington, and M. J. Smyth. 2015. DNAM-1 expression marks an alternative program of NK cell maturation. *Cell Rep.* 11: 85–97.
49. André, P., C. Denis, C. Soulas, C. Bourbon-Caillet, J. Lopez, T. Arnoux, M. Bléry, C. Bonnafous, L. Gauthier, A. Morel, et al. 2018. Anti-NKG2A mAb is a checkpoint inhibitor that promotes anti-tumor immunity by unleashing both T and NK cells. *Cell* 175: 1731–1743.e13.
50. Pfefferle, A., B. Jacobs, H. Netskar, E. H. Ask, S. Lorenz, T. Clancy, J. P. Goodridge, E. Sohlberg, and K.-J. Malmberg. 2019. Intra-lineage plasticity and functional reprogramming maintain natural killer cell repertoire diversity. *Cell Rep.* 29: 2284–2294.e4.
51. Enqvist, M., E. H. Ask, E. Forslund, M. Carlsten, G. Abrahamsen, V. Béziat, S. Andersson, M. Schaffer, A. Spurkland, Y. Bryceson, et al. 2015. Coordinated expression of DNAM-1 and LFA-1 in educated NK cells. *J. Immunol.* 194: 4518–4527.
52. Bryceson, Y. T., M. E. March, H.-G. Ljunggren, and E. O. Long. 2006. Synergy among receptors on resting NK cells for the activation of natural cytotoxicity and cytokine secretion. *Blood* 107: 159–166.
53. Zhang, Z., N. Wu, Y. Lu, D. Davidson, M. Colonna, and A. Veillette. 2015. DNAM-1 controls NK cell activation via an ITT-like motif. *J. Exp. Med.* 212: 2165–2182.
54. Busselaar, J., S. Tian, H. van Eenennaam, and J. Borst. 2020. Helpless priming sends $CD8^+$ T cells on the road to exhaustion. *Front. Immunol.* 11: 592569.
55. Yamamoto, H., T. Kishimoto, and S. Minamoto. 1998. NF-kappaB activation in CD27 signaling: involvement of TNF receptor-associated factors in its signaling and identification of functional region of CD27. *J. Immunol.* 161: 4753–4759.
56. Peperzak, V., Y. Xiao, E. A. M. Veraar, and J. Borst. 2010. CD27 sustains survival of CTLs in virus-infected nonlymphoid tissue in mice by inducing autocrine IL-2 production. *J. Clin. Invest.* 120: 168–178.
57. Joncker, N. T., N. C. Fernandez, E. Treiner, E. Vivier, and D. H. Raulet. 2009. NK cell responsiveness is tuned commensurate with the number of inhibitory receptors for self-MHC class I: the rheostat model. *J. Immunol.* 182: 4572–4580.
58. Tu, M. M., A. B. Mahmoud, A. Wight, A. Mottashed, S. Bélanger, M. M. A. Rahim, E. Abou-Samra, and A. P. Makrigiannis. 2014. Ly49 family receptors are required for cancer immunosurveillance mediated by natural killer cells. *Cancer Res.* 74: 3684–3694.
59. Kallies, A., and K. L. Good-Jacobson. 2017. Transcription factor T-bet orchestrates lineage development and function in the immune system. *Trends Immunol.* 38: 287–297.
60. Werneck, M. B. F., G. Lugo-Villarino, E. S. Hwang, H. Cantor, and L. H. Glimcher. 2008. T-bet plays a key role in NK-mediated control of melanoma metastatic disease. *J. Immunol.* 180: 8004–8010.
61. Malaisé, M., J. Rovira, P. Renner, E. Eggenhofer, M. Sabet-Baktach, M. Lantow, S. A. Lang, G. E. Koehl, S. A. Farkas, M. Loss, et al. 2014. KLRG1+ NK cells protect T-bet-deficient mice from pulmonary metastatic colorectal carcinoma. *J. Immunol.* 192: 1954–1961.
62. Lowin-Kropf, B., B. Kunz, F. Beermann, and W. Held. 2000. Impaired natural killing of MHC class I-deficient targets by NK cells expressing a catalytically inactive form of SHP-1. *J. Immunol.* 165: 1314–1321.
63. Felices, M., T. R. Lenvik, D. E. M. Ankarlo, B. Foley, J. Curtsinger, X. Luo, B. R. Blazar, S. K. Anderson, and J. S. Miller. 2014. Functional NK cell repertoires are maintained through IL-2Rα and Fas ligand. *J. Immunol.* 192: 3889–3897.
64. Fehniger, T. A., S. F. Cai, X. Cao, A. J. Bredemeyer, R. M. Presti, A. R. French, and T. J. Ley. 2007. Acquisition of murine NK cell cytotoxicity requires the translation of a pre-existing pool of granzyme B and perforin mRNAs. *Immunity* 26: 798–811.
65. Mortier, E., T. Woo, R. Advincula, S. Gozalo, and A. Ma. 2008. IL-15Ralpha chaperones IL-15 to stable dendritic cell membrane complexes that activate NK cells via trans presentation. *J. Exp. Med.* 205: 1213–1225.
66. Marçais, A., and T. Walzer. 2014. mTOR: a gate to NK cell maturation and activation. *Cell Cycle* 13: 3315–3316.